NeuroImage: Clinical 32 (2021) 102868

Contents lists available at ScienceDirect

NeuroImage: Clinical

journal homepage: www.elsevier.com/locate/ynicl

Subtle alterations in neonatal neurodevelopment following early or late exposure to prenatal maternal immune activation in mice

Elisa Guma [a,b,*], Emily Snook [a,d], Shoshana Spring [e], Jason P. Lerch [e,f,g,h], Brian J. Nieman [e,g,i,j], Gabriel A. Devenyi [a,c], M. Mallar Chakravarty [a,b,c,k,*]

[a] Computational Brain Anatomy Laboratory, Cerebral Imaging Center, Douglas Mental Health University Institute, Montreal, Quebec, Canada
[b] Integrated Program in Neuroscience, McGill University, Montreal, Quebec, Canada
[c] Department of Psychiatry, McGill University, Montreal, Quebec, Canada
[d] Department of Medicine, University of Toronto, Toronto, Ontario, Canada
[e] Mouse Imaging Centre, The Hospital for Sick Children, Toronto, Ontario, Canada
[f] Department of Neurosciences and Mental Health, The Hospital for Sick Children, Toronto, Ontario, Canada
[g] Department of Medical Biophysics, University of Toronto, Toronto, Ontario, Canada
[h] Wellcome Centre for Integrative Neuroimaging, University of Oxford, Oxford, United Kingdom
[i] Translational Medicine, The Hospital for Sick Children, Toronto, Ontario, Canada
[j] Ontario Institute for Cancer Research, Toronto, Ontario, Canada
[k] Department of Biological and Biomedical Engineering, McGill University, Montreal, Quebec, Canada

ARTICLE INFO

Keywords:
Maternal immune activation
Magnetic resonance imaging
Neonate brain development
Environmental risk factor
Ultrasonic vocalizations

ABSTRACT

Prenatal exposure to maternal immune activation (MIA) is a risk factor for a variety of neurodevelopmental and psychiatric disorders. The timing of MIA-exposure has been shown to affect adolescent and adult offspring neurodevelopment, however, less is known about these effects in the neonatal period. To better understand the impact of MIA-exposure on neonatal brain development in a mouse model, we assess neonate communicative abilities with the ultrasonic vocalization task, followed by high-resolution *ex vivo* magnetic resonance imaging (MRI) on the neonatal (postnatal day 8) mouse brain. Early exposed offspring displayed decreased communicative ability, while brain anatomy appeared largely unaffected, apart from some subtle alterations. By integrating MRI and behavioural assays to investigate the effects of MIA-exposure on neonatal neurodevelopment we show that offspring neuroanatomy and behaviour are only subtly affected by both early and late exposure. This suggests that the deficits often observed in later stages of life may be dormant, not yet developed in the neonatal period, or not as easily detectable using a cross-sectional approach.

1. Introduction

In utero exposure to maternal infection is an environmental risk factor for neurodevelopmental and psychiatric disorders in exposed offspring (Brown et al., 2001; Brown et al., 2004; Selten et al., 1997). Maternal response to infection involves an increase in circulating proinflammatory cytokines. Although adaptive in terms of maternal health, this response may have unwanted consequences by interfering with the regulatory roles of these immune molecules in the developing fetal brain (Choi et al., 2016; Gumusoglu and Stevens, 2019; Solek et al., 2018; Boksa, 2010; Thion et al., 2018). Importantly, both maternal immune responsiveness and neurodevelopmental processes in the fetus vary across gestation; thus, the timing of maternal immune activation (MIA)-exposure in gestation may influence the nature and severity of anatomical and behavioural disruptions in offspring (Reisinger et al., 2015). Identifying which gestational windows are most sensitive may be critical to our understanding of the effects of MIA-exposure.

Previously, our group has shown that the gestational timing of MIA-exposure has a differential impact on offspring neuro- and behavioural development at different developmental stages using the mouse as a model species. In the embryo brain, we observed striking brain volume increases following MIA-exposure late in gestation (gestational day [GD]-17), while exposure in early gestation (GD9) resulted in more focal volumetric decreases (Guma et al., 2021). In our investigations of brain development trajectories from adolescence to adulthood, we observed early MIA-exposure to induce greater neuroanatomical and behavioural

* Corresponding authors at: Cerebral Imaging Center, Douglas Mental Health University Institute, 6875 Boulevard LaSalle, Montreal, QC H4H 1R3, Canada.
E-mail addresses: elisa.guma@mail.mcgill.ca (E. Guma), mallar.chakravarty@mcgill.ca (M.M. Chakravarty).

https://doi.org/10.1016/j.nicl.2021.102868
Received 12 August 2021; Received in revised form 25 October 2021; Accepted 26 October 2021
Available online 29 October 2021

alterations than either late exposure or saline exposure, particularly in adolescence and early adulthood (Guma et al., 2021). This raises the question of what processes are occurring throughout the period between the embryo and childhood; namely: the neonatal period. Importantly, we previously identified this developmental window as being understudied and receiving less attention in the MIA neuroimaging literature (Guma et al., 2019).

Human neuroimaging evidence provides additional motivation for studying the neonatal period in more detail. Recent neonatal neuroimaging studies have found that *in utero* exposure to increased maternal inflammation (measured with either interleukin 6 or C-reactive protein) was associated with alterations to both functional and structural connectivity in the infant brain and toddler executive function (Graham et al., 2018; Rudolph et al., 2018; Spann et al., 2018). Some evidence of altered neonatal development following MIA-exposure exists in the animal literature as well. Positron emission tomography studies of the neonatal rabbit brain report increased neuroinflammation, as measured by TSPO, in MIA-exposed kits at postnatal day (PND) 1 and sustained until PND 17 (Zhang et al., 2018). MRI studies of MIA-exposed rhesus monkeys have also reported accelerated brain growth driven by white matter expansion in the first two years of life (Bauman et al., 2013) as well as grey matter reductions detectable at 1 year of age in a different study (Short et al., 2010). Finally, rodent studies of MIA-exposure have reported whole-brain and hippocampal volume alteration in the early postnatal period (PND 2–16) following Zika virus exposure (Patel et al., 2021), while no brain volume differences have been observed following GD 15 poly I:C-exposure in rats at PND 21 (Wood et al., 2019 Jan). Even though some observations in early phases of life exist (Bauman et al., 2013; Canales et al., 2021; Smolders et al., 2015; Fatemi et al., 2009), further work is required to understand the neurodevelopmental sequelae in the neonatal period following MIA-exposure, as this is a plastic window of brain development is important for putative intervention.

To examine this sensitive period we employ high-resolution *ex vivo* structural magnetic resonance imaging (MRI), a technique with comparable signal across species (Barron et al., 2021) to examine the effects of *in utero* exposure to early (GD 9) or late (GD 17) MIA with the viral mimetic, polyinosinic:polycytidylic acid (poly I:C), on the neonate (PND 8) brain. We also assayed neonate communicative ability using the ultrasonic vocalization (USV) task to phenotype neonatal mice at PND 8. Mouse pups typically start emitting USVs, or calls to their mother, to elicit pup retrieval by the dam, and other maternal care behaviours. These calls can be recorded based on frequency, number, and uration, in order to assess communication ability and adaptive behaviour (Scattoni et al., 2009).

1.1. Materials and methods

1.1.1. Animals, prenatal immune activation, and sample preparation

Pregnant dams were bred in our animal facility using timed mating procedures in female and male C57BL/6J mice (Thion et al., 2018; Reisinger et al., 2015; Guma et al., 2021; Guma et al., 2021; Guma et al., 2019) (described in Supplement 1.1). Pregnant dams were randomly assigned to one of four treatment groups (Fig. 1 for experimental design): (Brown et al., 2001) poly I:C (P1530-25MG polyinosinic:polycytidylic acid sodium salt TLR ligand tested; Sigma Aldrich) (5 mg/kg, intraperitoneally) at GD 9 (POL E; 6 dams), (Brown et al., 2004) 0.9% sterile NaCl solution at GD 9 (SAL E; 5 dams), (Selten et al., 1997) poly I:C at GD 17 (POL L; 6 dams), or (Choi et al., 2016) saline at GD 17 (SAL L; 4 dams). Since behavioural data can be more variable than structural brain anatomy, pups from each entire litter were tested on the USV task to maximize data availibility per litter . Following behavioural testing, all pups were perfused for brain collection, however, only the best perfused brains were selected for MRI scanning, resulting in a subset of each litter. We included between 2 and 3 males and females per litter, totaling 4–6 on average, with the exception of a few litters (3 litters had $<$ 4 pups due to perfusion quality , and 3 litters had more than 6 pups to account for the smaller litters . All procedures were approved by McGill University's Animal Care Committee under the guidelines of the Canadian Council on Animal Care.

Neonatal Sample Preparation for MRI: On PND 8, ~1 h following behavioural testing (see section 2.3) neonates were perfused first with 20 mL of 1X PBS, 2% gadolinium, and 1 μL/mL heparin (1000 USP units/mL) to remove any blood from the circulatory system, followed by 20 mL of 4% PFA with 2% gadolinium in PBS solution. Skulls were dissected and stored in a PBS solution with 4% PFA and 2% gadolinium for 24 h, after which they were transferred to a 0.02% Sodium Azide 1x PBS solution for long-term storage until scanning (see Supplement 1.2 for more detail; sample numbers in Table 1). Immunostimulatory potential of poly I:C was confirmed in separate dams (Supplement 1.1, 2.1, Supplementary table 1) data from (Guma et al., 2021).

1.2. Magnetic resonance image acquisition and processing

All samples were shipped to the Mouse Imaging Centre (Toronto, ON) for MRI scanning. A multi-channel 7.0-T MRI scanner with a 40 cm diameter bore (Varian Inc., Palo Alto, CA) was used to acquire anatomical images of the neonate brains within skulls. A custom-built 16-coil solenoid array was used to acquire 40 μm^3 resolution images from 16 samples concurrently (Dazai et al., 2011; Lerch et al., 2011) (see Supplement 1.4 for details).

Preprocessed neonate brain images of all subjects in the study were aligned by unbiased deformation based morphometry using the antsMultivariateTemplateConstruction2.sh tool (https://github.com/CoBrALab/twolevel_ants_dbm) (Avants et al., 2011). The output of this iterative group-wise registration procedure is a study average against which groups can be compared, as well as deformation fields that map each individual subject to the average at the voxel level. Relative log-transformed Jacobian determinants (Chung et al., 2001), which explicitly model only the non-linear deformations and remove global linear transformation (attributable to differences in total brain size) were blurred at 160 μm full-width-at-half-maximum to better conform to Gaussian assumptions for downstream statistical testing.

1.3. Behavioural testing: Ultrasonic vocalization task

Isolation-induced ultrasonic vocalizations of neonate offspring were assessed with standard procedures (Fernández, 2017; Baharnoori et al., 2012). This test was selected because, apart from motor abilities, it is one of the few complex behaviours that can be assessed this early in mouse development (Feather-Schussler et al., 2016; Branchi and Ricceri, 2002) and because communicative abilities are a core deficit of ASD (Inui et al., 2017). Testing was performed using the Noldus UltraVox™ system (Noldus Information Technology, Leesburg, VA) on PND 8, as the rate of calling peaks around this time in mouse pups (Scattoni et al., 2009). Duration of each individual call per session per animal were recorded as raw data, as were the following summary measures per animal: total number of calls, maximum and minimum duration of calls, maximum and minimum call interval. For simplicity, call duration (and mean duration) was the only measure analyzed and discussed. See Table 1 for sample size, and Supplement 1.5 for details.

1.4. Statistical analyses

1.4.1. Neuroimaging data analysis

Statistical analyses were performed using the R software package (R version 3.5.1, RMINC version 1.5.2.2 www.r-project.org). First, we confirmed that there were no statistically significant differences between our two control groups (SAL E and SAL L), which allowed us to combine them into a single group, leaving us with three groups: SAL, POL E, and POL L, consistent with our previous work (Guma et al.,

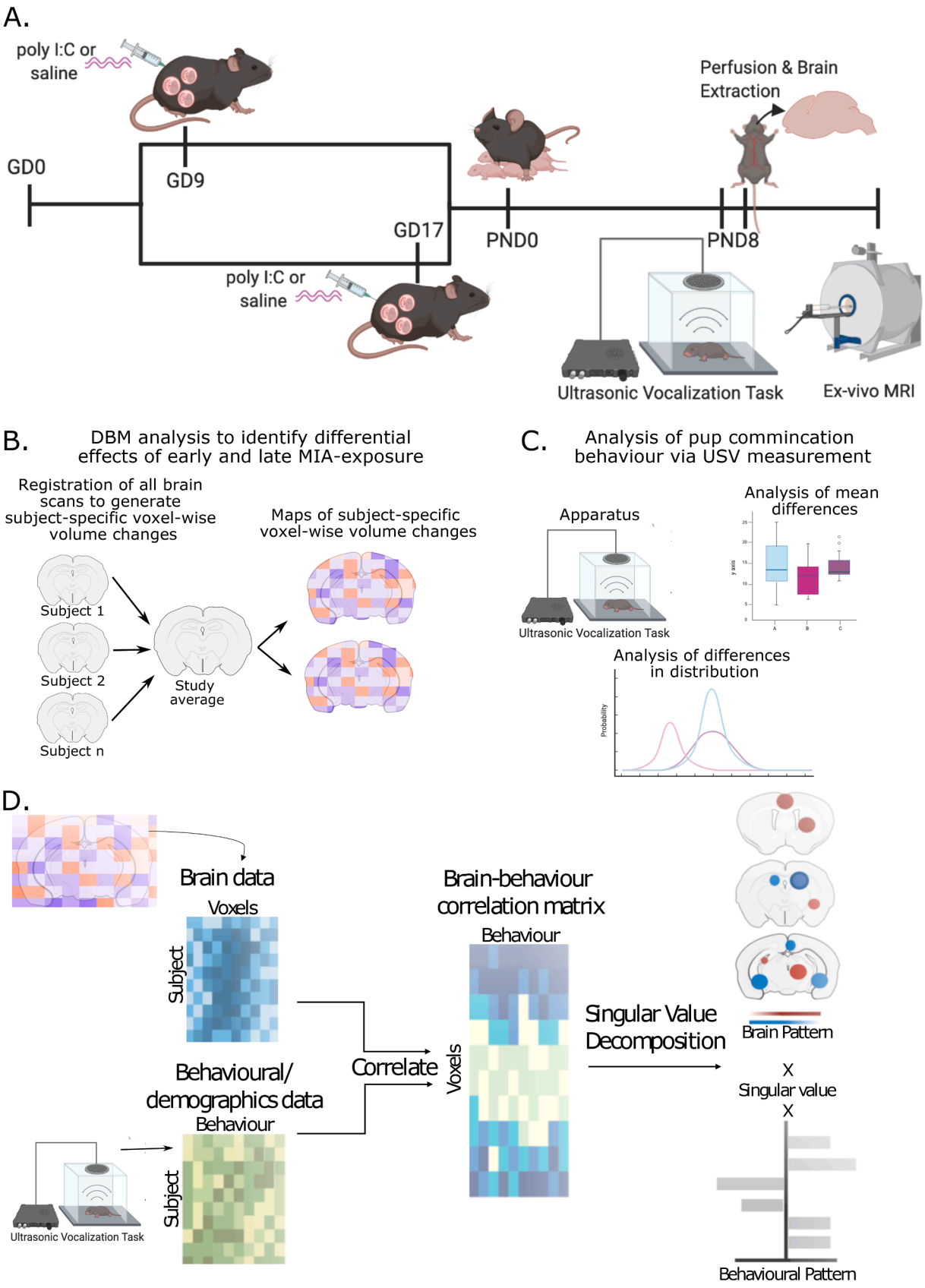

Fig. 1. Experimental timeline. A. Pregnant dams were injected on either GD 9 or 17 with either poly I:C or vehicle . On PND 8 offspring were tested on the ultrasonic vocalization task (USV) to assess communicative behaviour. Following behaviour, mice were perfused, and brains were prepared for *ex-vivo* MRI. B. Analysis flow of deformation-based morphometry analysis used to detect voxel-wise brain volume differences due to early or late MIA-exposure. C. Analysis of USV for mean differences in call duration and frequency, and differences in distribution of calls. D. Multivariate analysis of brain-behavior data using partial least squares (PLS) analysis to identify patterns of covariation.

Table 1
Final sample size neonate MRI acquisition and neonate USV data following quality control.

Group	Males (MRI)	Females (MRI)	Males (USV)	Females (USV)	Litters	# of pups per litter (median [range])
SAL E	7	9	13	10	5	7 [2–8]
SAL L	8	11	14	16	4	9 [5–9]
POL E	13	13	23	17	6	7 [5–8]
POL L	16	13	25	14	6	8 [3–10]

2021). To assess the effects of poly I:C exposure either early or late in gestation on neonatal neuroanatomy, we ran a whole-brain voxel-wise linear mixed-effects model (lme4_1.1–21 package; (Bates et al., 2015) on the relative Jacobian determinant files using group and sex as fixed effects, and number of pups per litter (ranging from 2 to 10; Table 1) as random intercepts. The litter size was selected as a random effect as it may have significantly affect development in early phases of life (Jiménez and Zylka, 2021); since we do not cull litters to be the same size, we considered this an important factor to control. The False Discovery Rate (FDR) correction was applied to correct for multiple testing (Supplement 1.6.1 for details). This analysis was run again with the POL L group as the reference in order to directly compare POL E to POL L differences. Sex-by-group interactions were explored as a follow up analysis as described in Supplement 1.6.1 and Supplement 2.2.2.

1.4.2. USV data analysis

Since there were no differences in group means (see Supplement 1.6.2 for analysis details), we used a hierarchical shift function in order to maximize the data collected for each mouse (Rousselet et al., 2017). This allows us to quantify how two distributions differ based on deciles of the distributions, i.e. it describes how each decile should be shifted to match one distribution to another. When a significant difference is observed between deciles it suggests that there is a specific difference in the number of calls between groups at a specific call length; this allows us to determine whether differences are consistent across the entire distribution, or more localized to one or both tails, or the center. Three pairwise comparisons were made (SAL - POL E, SAL - POL L, POL L - POL E) on the distributions for the duration for each call for each animal in the 5 min recording period, thresholded between 5 ms and 300 ms (a range previously used to filter out noise (Scattoni et al., 2009). A percentile bootstrap technique was used to derive confidence intervals based on differences in distribution at each decile of the distribution. This was then repeated to assess sex differences: the same comparisons were made in only males, and only females, followed by the same percentile bootstrap procedure. Sex differences were also investigated in the same way with the same pairwise comparisons as above for males and females separately.

1.4.3. Partial least squares analysis

A partial least squares (PLS) analysis, previously applied by our group (Guma et al., 2021), was used to investigate putative brain-behaviour relationships between neonate neuroanatomy and USV behaviour. This is a multivariate technique for relating two sets of variables to each other by finding the optimal weighted linear combinations of variables that maximally covary with each other (Zeighami et al., 2019; McIntosh and Mišić, 2013; McIntosh and Lobaugh, 2004). The two variables used in this study were voxel-wise brain volumes (brain matrix) and USV call duration binned by decile of distribution (based on length), as well as sex, and number of pups per litter (described in Table 1) (behaviour/demographics matrix). The behaviour matrix was z-scored and correlated to the brain matrix to create a brain-behaviour covariance matrix. A singular value decomposition was applied to generate a set of orthogonal latent variables (LVs), which describe linked patterns of covariation between the input brain and behaviour matrices. Permutation testing and bootstrap resampling were applied to assess LV significance and reliability (further details in Supplement 1.6.3).

2. Results

2.1. Subtle neuroanatomical differences in neonate brain anatomy

Linear mixed-effects analysis of voxel wise volume difference revealed extremely subtle differences between SAL and POL E offspring ($t = 4.47$, <20%FDR) wherein POL E offspring had a larger volume of a subregion of the right lateral amygdalar nucleus, a larger cluster of voxels in the right ventral hippocampus, and a smaller cluster of voxels in the right entorhinal cortex (Fig. 2).

POL L offspring had more significant, yet focal changes relative to the SAL offspring ($t = 5.47$, <1%FDR). Larger volume in a cluster of voxels within the right prelimbic area, left amygdala, right insula, and right Crus I of the cerebellum was observed in the POL L offspring. Conversely, volume decreases were observed within a subregion of the left corpus callosum and right fimbria, two white matter tracts , as well as the right ventral subiculum and left globus pallidus in the POL L group (Fig. 2). These results (brain maps) are shown at a less stringent threshold in Supplement 2.2.1 and Supplementary Fig. 2).

Finally, relative to the POL E group, the POL L group had smaller volume in subregions of the right striatum and larger volume in subregions of the left amygdala and right periaqueductal gray at a moderate significance threshold ($t = 4.80$, <10%FDR) (Fig. 2).

Post-hoc investigation of sex differences revealed subtle effects in the POL L group relative to SAL ($t = 4.23$, <20%FDR); in the medial septum, pontine reticular nucleus, and cerebellum, volume for male POL L offspring was smaller than SAL, whereas the opposite was true for females, with larger volume for POL L than SAL offspring (Supplement 2.2.2 and Supplementary Fig. 3). Additionally, the main effect of sex is represented in Supplementary Fig. 4 ($t = 4.89$, <1%FDR) in which we detect canonical sex differences in regions such as the medial preoptic area, the bed nucleus of the stria terminalis, and the medial amygdala (larger volume in males); these are similar to previously identified sex differences in the neonatal mouse brain using MRI (Qiu et al., 2018). This suggests that we are sensitive to both profound and subtle changes, due to sex or MIA-exposure respectively.

2.2. Neonate ultrasonic vocalization behaviour results

No overall difference in mean call duration was observed in the ultrasonic vocalization data, however, data distribution and variance appeared different between groups. To better investigate potential differences in call duration, distributions for all calls made in the recording period, rather than mean call duration, were compared using the shift functions (Fig. 3A and Supplement 2.3). The shift function revealed significant differences in distribution of call length between the SAL and POL E groups (Fig. 3B). POL E offspring made significantly fewer calls at each decile of call length suggesting that overall, they made shorter calls; more subtle differences were observed for deciles for shorter calls (decile 1, $p = 0.035$, decile 2, $p = 0.003$), and greater differences for longer duration calls ($p < 0.00001$) (Fig. 3C). The difference per decile is outlined in Supplementary Table 2. Similar differences were observed between POL L and POL E offspring, again with POL E making significantly shorter calls identified by the shifted distribution, with the most significant differences observed for long calls (Supplementary Table 4) (Fig. 3E). Finally, there was no significant difference in distribution of call length between POL L and SAL offspring at any of the deciles (Supplementary Table 5) (Fig. 3D). The distribution for the duration of all calls, and mean call duration are shown for each individual litter Supplementary Fig. 5, as is the variance (Supplementary Table 3). Investigation of possible sex differences revealed that POL E females made significantly fewer long call across all deciles than SAL females, while there were no differences between POL E males and SAL males.

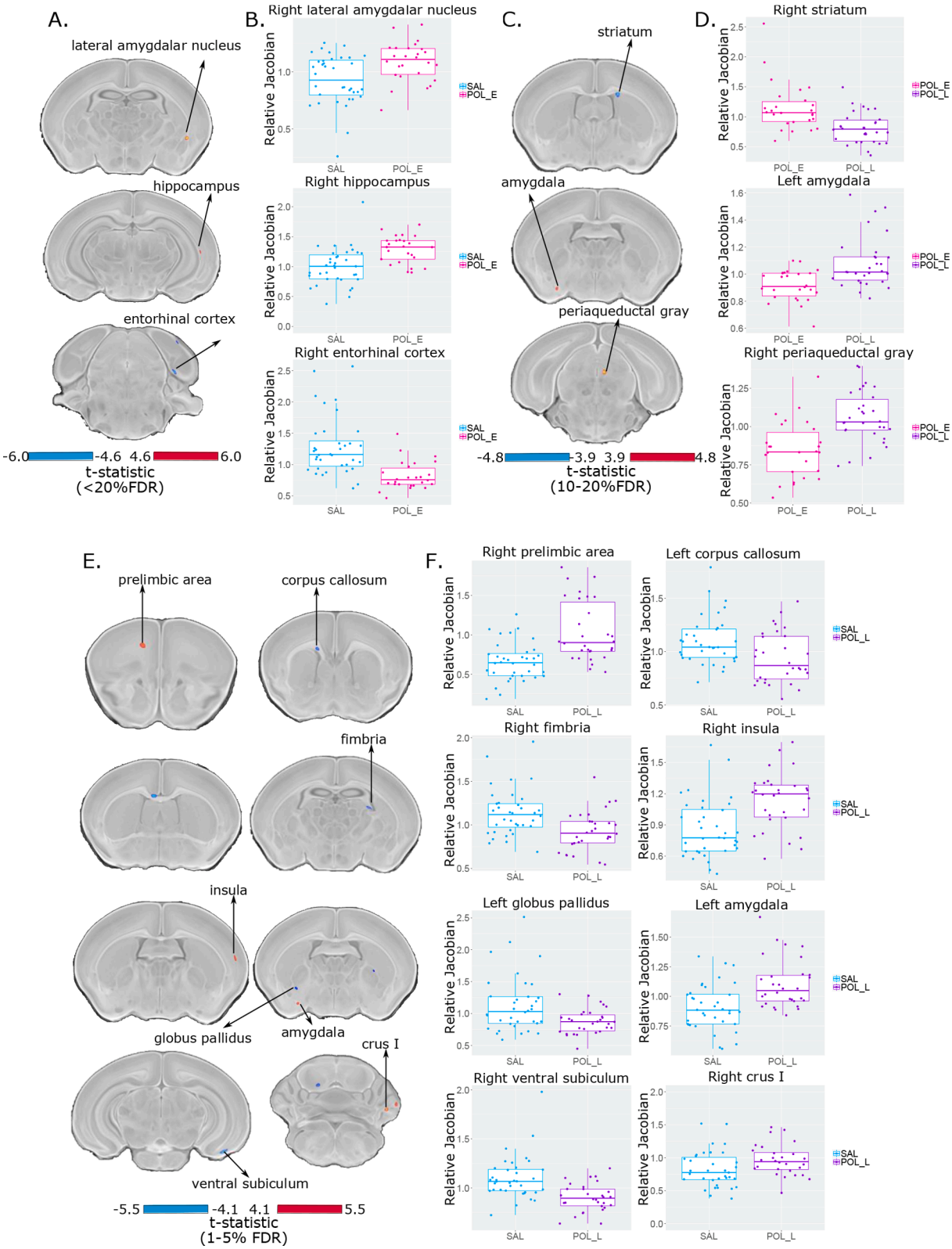

Fig. 2. Neuroanatomical changes in the PND 8 neonate brain following GD 9 (A and B) or GD 17 (C and D) exposure. A. t-statistic map of group (POL E vs SAL) thresholded at 20% (bottom, t = 4.60 to max, top, t = 6.00) overlaid on the study average. B. Boxplot of peak voxels (voxels within a region of volume change showing largest effect) selected from regions of interest highlighted in A. C. t-statistic map of group (POL L vs POL E) thresholded at 20% (bottom, t = 3.9) and 10% FDR (top, t = 4.8) overlaid on the study average with peak voxels plotted in D. E. t-statistic map of group (POL L vs SAL) thresholded at 5% (bottom, t = 4.10) and 1% FDR (top, t = 5.50) overlaid on the study average with peak voxels plotted in F.

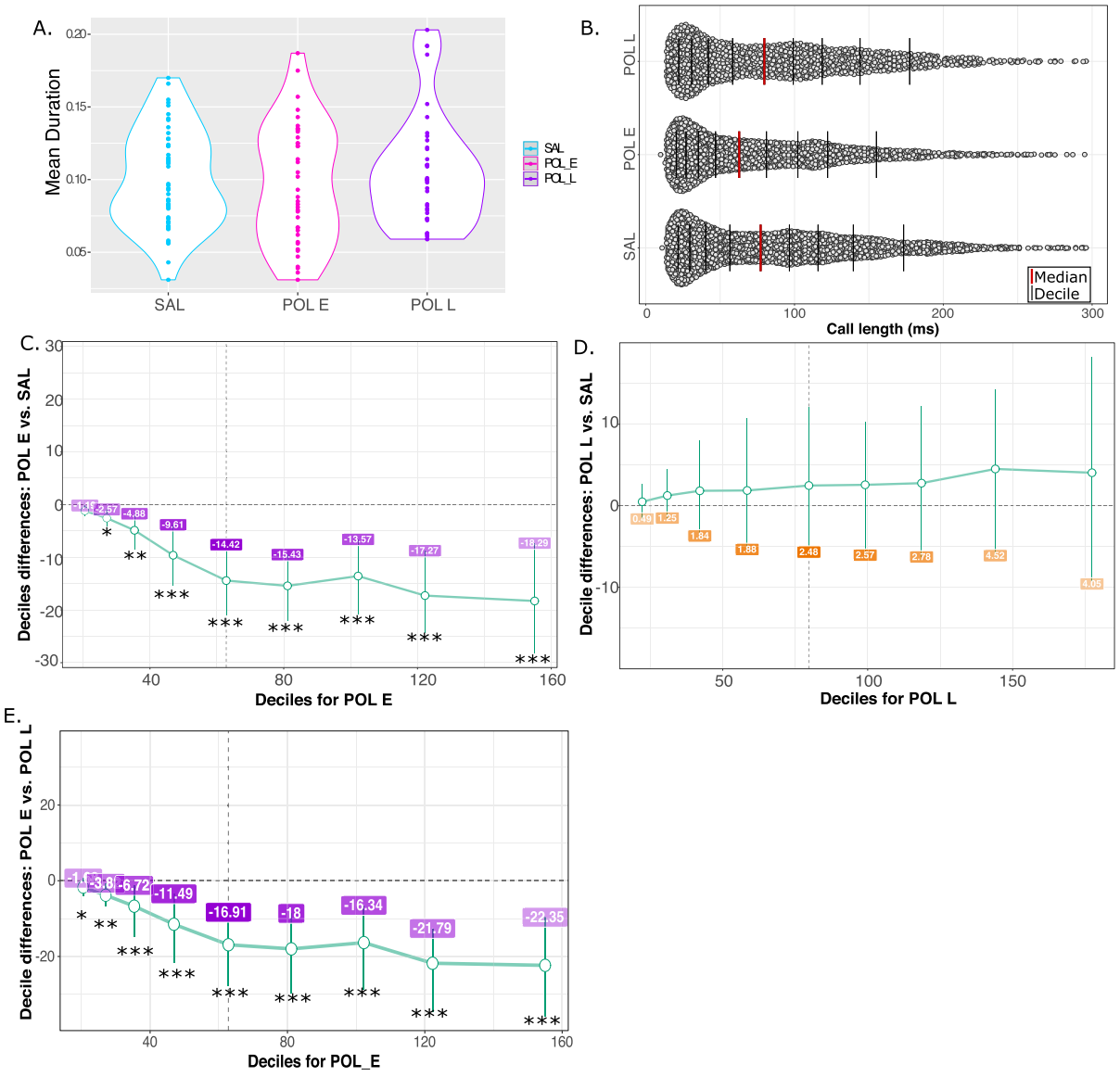

Fig. 3. Results for ultrasonic vocalizations. A. Violin plot for mean call duration for each group (SAL, POL E, POL L) showing no overall differences in mean. B. Distribution of call length (ms) for all calls made by all mice per group in the 5-minute recording period. The red line identifies the median of the data, while each black bar denotes a decile of distribution. C. Percentile bootstrapping technique applied to identify the difference in decile between the POL E group and SAL, showing significantly fewer calls made by the POL E group across the range of distributions. D. Percentile bootstrapping analysis reveals no significant difference between distributions for POL L relative to SAL as error bars cross the zero line. E. Percentile bootstrapping analysis reveals significantly fewer calls for POL E group relative to POL L across all deciles. *p < 0.05, **p < 0.01, ***p < 0.001. (For interpretation of the references to color in this figure legend, the reader is referred to the web version of this article.)

Conversely, POL L females made significantly more calls than SAL females across most deciles of distribution, while no differences were observed in males (Supplement 2.4 and Supplementary Fig. 6).

2.3. Neonate USV-brain PLS

PLS analysis of voxel-level volume changes and USV call frequency binned into deciles (as with the distribution analysis) yielded three significant latent variables (LV)s. The first accounted for 46% covariance between matrices (p = 0.003) (Fig. 4A). This showed a pattern of increased call frequency associated with larger volume in the left thalamus, left lateral septum, left auditory cortex, left ventral hippocampus, and fourth ventricle, and smaller volume in the right primary motor and somatosensory cortex, right amygdala, right and left corpus callosum, right and left thalamus (Fig. 4BC). The three groups load similarly onto the latent variable, with Pearson's correlation coefficient, R, as follows: SAL = 0.606; POL E = 0.539; POL L = 0.760. Thus, it seems as though the POL L group expressed the patterns most strongly, while the POL E group least strongly (Fig. 4D). The second LV accounted for 23% of the covariance (p = 0.04) (Fig. 4E) describing a pattern of increased corpus callosum, cingulate cortex, and subiculum volume, decreased thalamic and cerebellar volume associated with a greater number of shorter calls, and female sex (Fig. 4FG). Again, the three groups load similarly (R: SAL = 0.748; POL E = 0.535; POL L = 0.711), however, the correlation coefficient is lower in the POL E than the POL L and SAL groups (Fig. 4H). Finally, the third LV is described in Supplement 2.5 and Supplementary Fig. 7 since it only accounted for 10% of the covariance (p = 0.02) and the brain-behaviour covariation did not differentiate between groups (R = SAL = 0.762; POL E = 0.696; POL L = 0.747). Brain and behaviour loadings are plotted separately per group in Supplementary Fig. 8).

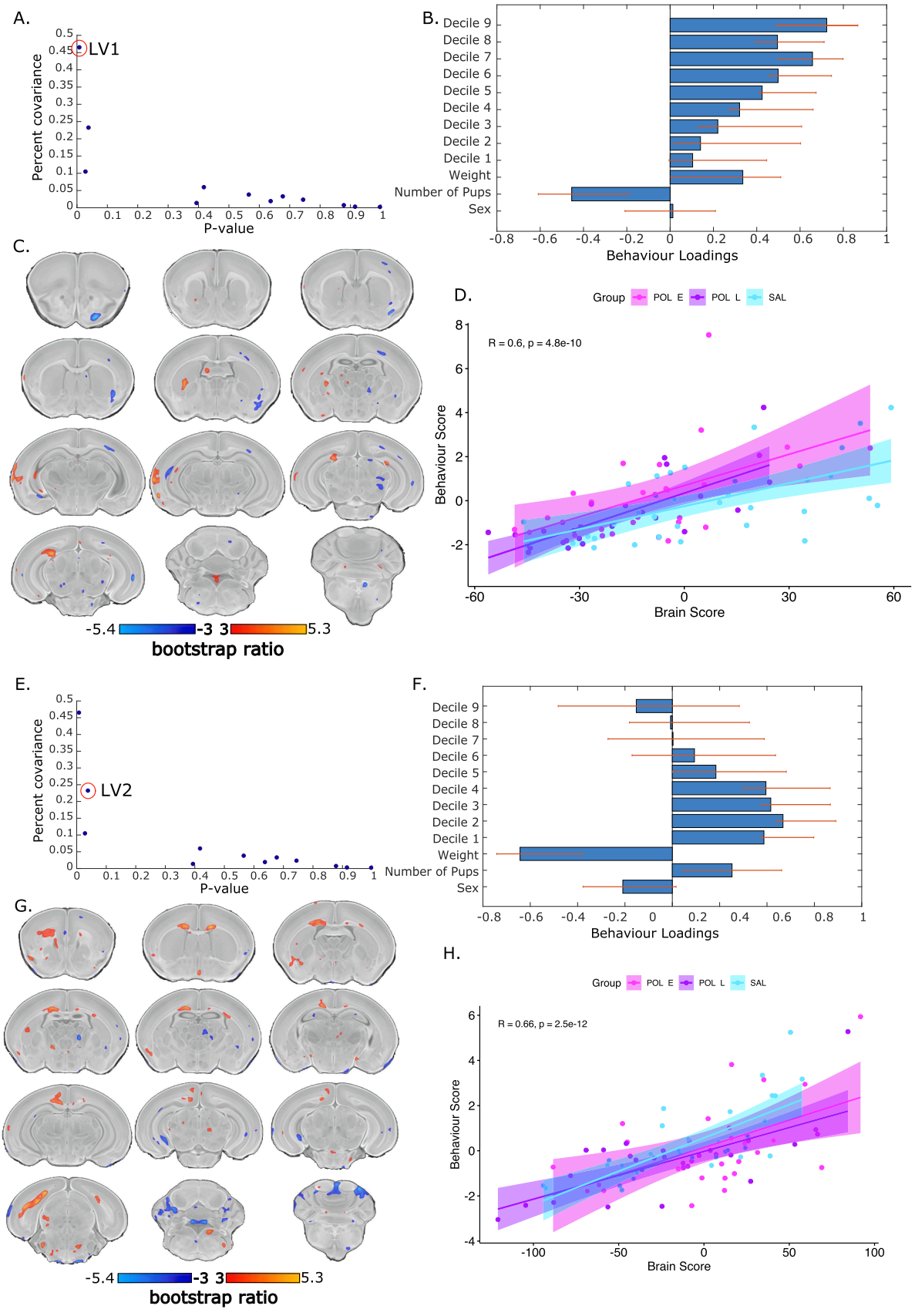

(caption on next page)

Fig. 4. Partial least squares (PLS) analysis results for first and second significant latent variables (LV). A. Covariance explained (y-axis) and permutation p-values (x-axis) for all 12 LVs in the PLS analysis. LV1 is circled in red ($p = 0.003$, %covariance = 46%). B. Behaviour weight for each decile of distribution for the USV calls included in the analysis showing how much they contribute to the pattern of LV1. Singular value decomposition estimates the size of the bars whereas confidence intervals are estimated by bootstrapping. Bars with error bars that cross the 0 line should not be considered as significantly contributing to the LV. C. Brain loading bootstrap ratios for the LV1 deformation pattern overlaid on the population average, with positive bootstrap ratios in orange yellow (indicative or larger volume), and negative in blue (indicative of smaller volume). Colored voxels make significant contributions to LV1. D. Correlation of individual mouse brain and behaviour score, color coded by treatment group with a trend line per group. POL E offspring (magenta) express this pattern more strongly than SAL and POL L groups. E. LV2 is circled in red on the same plot as in A ($p = 0.04$, %covariance = 23%). Behaviour weights (F), brain weights (G), and brain-behaviour correlations (H) represented for LV2 as for LV1. (For interpretation of the references to color in this figure legend, the reader is referred to the web version of this article.)

3. Discussion

Studies investigating the long-term impact of MIA-exposure on offspring development have identified a number of neuroanatomical, cellular, and behavioural abnormalities associated with this risk factor; many of these alterations overlap with those identified in neurodevelopmental disorders such as schizophrenia and autism spectrum disorder (Knuesel et al., 2014; Estes and McAllister, 2016; Brown and Meyer, 2018). While the majority of rodent MIA models have reported abnormalities in adolescent or adult offspring, here we investigate the less studied neonatal period. Based on the early life emergence of neurodevelopmental disorders such as autism spectrum disorder, as well as data from other preclinical studies in the rabbit and rhesus monkey (Zhang et al., 2018; Bauman et al., 2013), we hypothesized that neuroanatomical and behavioural deficits due to MIA-exposure would already be detectable in the neonatal period. Further, we hypothesized the timing of MIA-exposure would modulate the severity of offspring outcomes based on variation in neurodevelopment, and our previous findings (Guma et al., 2021). We leveraged high-resolution *ex vivo* MRI to characterize the effects of MIA-exposure either early or late in gestation on neonatal brain anatomy in conjunction with an assay of communicative behaviours at PND 8.

Here, we observed subtle neuroanatomical changes due to MIA-exposure in the neonate at PND 8. In our previous investigations of MIA-exposure on brain development, we observed MRI-detectable volume changes in the embryo brain due to both early and late exposure using similar sample size and the same experimental procedure for MIA induction and breeding protocols (Guma et al., 2021) (see Fig. 5). For early exposed embryos (GD 9) volume reductions were observed in the hippocampus, globus pallidus, thalamus, and cerebellum, while volume increases were observed in the prelimbic area, lateral septum, subventricular zone, and caudate-putamen amongst others (Guma et al., 2021). In contrast, late exposed embryos (GD 17) had striking brain-wide volume increases, particularly in the basal ganglia, hippocampus, cortex, corpus callosum, thalamus, and cerebellum (Guma et al., 2021). Furthermore, we previously identified significant deviation in neurodevelopmental trajectories of early MIA-exposed offspring in the adolescent and early adult period, again with a similar sample size and the same experimental procedure for MIA induction, wherein accelerated volume increase, followed by a normalization were observed in the hippocampus, anterior cingulate cortex, striatum, and lateral septum, amongst other regions; in contrast, late-exposed offspring displayed only subtle deviations in trajectory (Guma et al., 2021). Thus, it is possible that the changes detected in the embryo brain are a result of acute remodeling in response to the increased inflammation *in utero*, but that these changes resolve in the neonatal period. The changes detected in the embryo period may be indicative of some latent disruptions that lead to aberrant neurodevelopment in later stages of adolescence and early adulthood. It is possible that the observations we made at PND 8 capture some crossing trajectories of aberrant neurodevelopment, as depicted in Fig. 5. In further support of this model, our longitudinal work suggests that the peak of change in brain volume due to MIA exposure may be in the adolescent/early adult period (PND 38–60) (Guma et al., 2021), a result supported by previously longitudinal work conducted in rats (Crum et al., 2017). Additionally, cross-sectional structural MRI studies in offspring exposed to poly I:C at either GD 12, 15, or 17 have also reported subtle structural alterations in adult offspring (Mueller et al., 2021; Kreitz et al., 2020), which supports the hypothesis that differences may begin to normalize later in development.

In contrast with our findings, brain imaging studies report neuroanatomical and functional changes associated with chronic exposure to inflammation *in utero* in human neonates (Graham et al., 2018; Rudolph et al., 2018; Spann et al., 2018). In addition to MIA-exposure, ASD may also be associated with alterations in neuroanatomy in the neonatal period, with differences detectable as early as 6 months of age (Shen and Piven, 2017). Furthermore, neonatal rhesus monkeys whose mothers

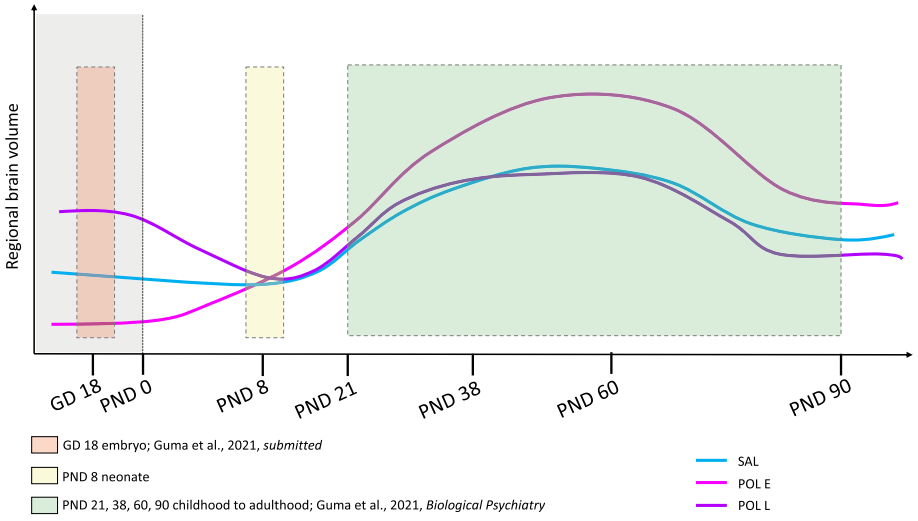

Fig. 5. Hypothetical neurodevelopmental trajectories for the three examined groups, SAL, POL E, and POL L based on the work presented in this manuscript (PND 8) as well as our previous investigation of GD 18 embryo brain volume (Guma et al., 2021) and longitudinal brain development from PND 21 to 90. The same experimental procedures and methodology was employed to induce MIA allowing for comparability between studies.

were exposed to maternal immunoglobulin G (isolated from human mothers whose children had been diagnosed with ASD) in the first two trimesters displayed acceleration in brain growth, driven by white matter expansion particularly in the frontal and occipital lobes, and displayed behavioural features parallel to ASD (Bauman et al., 2013). Similarly, prenatal influenza virus has been associated with grey matter volume reductions in 1 year old primate offspring (Short et al., 2010). MIA-exposure in late gestation in the rabbit has also been shown to increase neuroinflammation in the first two postnatal weeks of life (measured by TSPO PET imaging) (Zhang et al., 2018; Kannan et al., 2011), and to decrease cortical serotonin binding (Kannan et al., 2011). A recent MRI-based investigation of the effects of GD 18 Zika Virus exposure on mouse offspring development reported alterations to both whole-brain and hippocampal volume throughout the neonatal period, with decreased volume at PND 2, and increased volume at PND 16 (Patel et al., 2021). In contrast, the effects of poly I:C exposure at GD 15 were found to induce no neuroanatomical differences in rats later in development (PND 21) (Wood et al., 2019). Differences in the nature of MIA-exposure may explain some of these differences, as the human and first rhesus monkey study identified differences following more chronic inflammation. Differences in neurodevelopment between species could explain some of these discrepancies in findings (Kentner et al., 2019). Naturally, the relatively minor alterations here require further investigation at both the structural and functional levels.

To better understand how the timing of MIA-exposure may differentially impact neurodevelopment, it is important to consider the possible processes it may be interfering with. In the developing mouse brain, the neural tube forms, and neurogenesis begins at GD 9, corresponding with our early injection timing, and ends by GD15, prior to the late injection timepoint. Microglia also begin to colonize the brain at GD 9, making this developmental period sensitive to potential inflammatory insults such as those elicited by MIA (Thion et al., 2018; Wolf, 2013; Ginsberg et al., 2017). Thus, it is possible that MIA-exposure at GD9 may induce more lasting changes to cell proliferation and the development of the neuroinflammatory system. By GD 17, many neurodevelopmental processes are complete, however cortical cell migration and myelination are ongoing (Selemon and Zecevic, 2015). In the GD17-exposed neonates we did observe subtle volume alterations to cortical regions, such as the prelimbic and insular cortices, as well as white matter regions such as the corpus callosum and fimbria. Finally, PND 8, the age at which we evaluated offspring brain anatomy and behaviour, likely corresponds to a human infant at term as myelination and synaptogenesis are underway during this window (Semple et al., 2013).

Social and communicative deficits are central to the pathology of many neurodevelopmental disorders, such as ASD. We experimentally modeled these impairments by measuring ultrasonic vocalizations in our MIA-exposed neonates and found that early exposed groups made significantly fewer long calls which seem to be driven by the female offspring. Although the findings in the literature are fairly heterogeneous regarding the directionality of USV effects (i.e. increases or decreases due to MIA-exposure), previous groups have also observed decreases in neonatal vocalization in rodent MIA-models consistent with our findings (Baharnoori et al., 2012), as well as other animal models for neurodevelopmental disorders (Trezza, 2018; Malkova et al., 2012). Interestingly, some studies have also investigated putative sex-dependent differences in this behaviour but observed greater alterations in male exposed offspring rather than in females as we observed (Fernández, 2017; Gzielo et al., 2021).

Understanding the relationship between neuroanatomical abnormality and behaviour is critical and may be a useful avenue for understanding psychiatric disorders along dimensions rather than categories (Xia et al., 2018). We implement the multivariate technique, PLS, to investigate the relationship between voxel-level volume changes and USV call frequency. This allowed us to observe that neonates who made more frequent longer calls had a different brain anatomy than those that made more frequent shorter calls. Importantly, longer calls were associated with larger volume in the ventral hippocampus, lateral septum, auditory cortex, thalamus, and fourth ventricle and smaller volume in somatomotor cortices, corpus callosum, thalamus, and amygdala (based on the first latent variable with the highest covariance explained). In contrast, short calls were associated with larger volume in the corpus callosum, cingulate cortex, and subiculum, and smaller thalamic and cerebellar volume. Previous studies have found that neurotypical pup calls tend to be clustered in short sequences, thus, longer vocalizations may be indicative of some abnormal development or distress (Urbanus et al., 2020). Importantly, these patterns were similar between groups, with a slightly stronger expression in the POL L group and slightly weaker expression in the POL E group, an association requiring future investigation.

These results suggest that different brain regions may be involved in the production of short versus long vocalization. Further, some regions, such as the thalamus are implicated across all patterns, suggesting that it may play a central role in communicative abilities. In fact, vocalizations have been shown to involve the cortico-striatal-thalamic loops, as well as motor neurons in the cortex and brainstem (Arriaga and Jarvis, 2013). Although the specific cellular underpinnings of vocalization behaviour remain to be elucidated, previous work has shown that knocking out certain genes involved in social behaviour, and associated with ASD (such as neuroligin-3 or 4, SHANK3, and oxytocin, amongst others) can modulate vocalization behaviour in mice (Fischer and Hammerschmidt, 2011). Finally, some of these regions involved in these brain patterns have previously been implicated in MIA-exposure. The changes in the corpus callosum observed may be related to previous work showing that MIA at GD 17 has been associated with long lasting epigenetic changes in myelin stability genes and proteins in exposed offspring (Richetto et al., 2017). Furthermore, alterations to the volume of the lateral septum, somatomotor and cingulate cortices, and subiculum have been observed both in our previous work investigating the effects of MIA in adolescence (Guma et al., 2021) and that of others (Crum et al., 2017).

The results presented in this manuscript should be considered in light of their limitations. The strategy we employed, leveraging high-resolution *ex vivo* MRI (rather than longitudinal) was selected as we thought it would be more sensitive at detecting neuroanatomical differences in the brain of neonate mice prenatally exposed to MIA. We expected to find larger neuroanatomical alterations, but only recovered subtle, focal effects. We did observe more striking differences in neuroanatomy, particularly in the late-exposed offspring at a more lenient correction threshold, which may suggest that a larger sample size may be required to identify subtle differences in neuroanatomy at this developmental stage. Based on previous work by Lerch and colleagues (Lerch et al., 2012) we were sufficiently powered to detect a 3% volume change with 10 subjects per group. However, it is possible that the within-subject variability in the neonatal timepoint may be higher than in adulthood given the rapid rate at which the brain is developing. The coefficient of variation (standard deviation/mean) for voxel-wise brain volume does indeed show a higher range in the neonatal sample compared to the embryo sample (Guma et al., 2021) and to the adolescent timepoint from our longitudinal sample (Guma et al., 2021) (see Table 2). It is conceivable that a single timepoint here, when the brain is growing so rapidly, might be noisier due to very subtle differences in maturation rates that for the purposes of this study add to the noise (described in Supplement 1.6.1).

Table 2
Coefficient of variation presented as a range across all voxel-wise brain data from the neonate data (PND8) presented here as well as two previous publications (Guma et al., 2021; Guma et al., 2021).

	SAL	POL E	POL L
Embryo (GD18)	0 to 0.848	0 to 1.130	0 to 0.905
Neonate (PND8)	0 to 1.796	0 to 1.642	0 to 1.744
Adolescence (PND38)	0 to 0.520	0 to 0.448	0 to 0.468

To investigate potential regional differences, we plotted the maps for the coefficient of variation calculated at the voxel level for the neonate sample for each treatment group, and interestingly there is some regional variation in the variance observed. Regions with higher variance include the ventricles, some white matter tracts like the corpus callosum, as well as sections of the striatum and cerebellum (Supplementary Figure 8). Interestingly, the regions do not consistently overlap with regions in which we observed volumetric changes in the univariate analyses or the PLS. Furthermore, the regions with increased variation seem to be consistent across groups, suggesting that the exposure to MIA is not increasing the variation specifically, but that these differences may in fact be due to rapid neurodevelopmental processes. However, it is still possible that w they may be capturing differences in offspring susceptibility and resilience to the MIA-exposure; as previously shown, not all offspring are expected to be affected equally by poly I:C exposure (Mueller et al., 2021). Finally, it has been consistently shown that other variables related to housing, animal species as well as variance in poly I:C molecular weight could all introduce variability in findings (Kentner et al., 2019; Mueller et al., 2019). Although housing, and species were consistent throughout our studies, a new batch of poly I:C (albeit the same product from the same vendor) was used here, relative to our previously published work; although immunostimulatory potential was confirmed in a separate cohort (Supplementary Table 1), this may account for some differences in maternal immune response, physiology, and pregnancy outcomes (Kentner et al., 2019; Mueller et al., 2019).

In future work, employing longitudinal imaging on larger groups of offspring throughout the neonatal period may provide more sensitivity in detecting developmental changes rather than the cross-sectional approach employed here. This approach requires a significant amount of development, which our scanner was not equipped for at the time that this experiment was designed. This approach has been successful at uncovering sex differences throughout mouse brain development (Qiu et al., 2018), and in previous work by our group examining offspring development from weaning to adulthood (Guma et al., 2021). Employing analyses that leverage the network structure of the brain, such as the PLS included here, or structural covariance may be useful, as covariance patterns may allow for better integration of brain structure with functional and transcriptional expression patterns of the brain (Mueller et al., 2021). Furthermore, we only assayed communicative abilities, as this is one of the few complex behaviours testable in neonate mice. However, a more comprehensive assay of social and repetitive/stereotypic behaviours (tested later in offspring development) may provide a more complete examination of putative deficits relevant to ASD pathology (Amaral et al., 2008). Finally, although the results indicated more subtle brain structure changes than we had expected, this observation advances our understanding of MIA-exposure on brain development in light of changes reported from the embryonic (Guma et al., 2021) and adolescent/early adult periods (Guma et al., 2021).

In conclusion, we comprehensively examined the effects of prenatal MIA-exposure, a known risk factor for neuropsychiatric disorders, at two gestational timepoints on neonatal brain anatomy and behaviour. Neuroanatomical differences were mostly resolved by the neonatal period, where we observed deficits in communication in the early exposed offspring, again, with greater effects in female offspring. These findings show that MIA-exposure induces subtle changes to neonatal development, which may require further investigation, but aid in our understanding of how this risk factor increases the likelihood of developing neuropsychiatric illnesses later in life.

Declaration of Competing Interest

The authors declare that they have no known competing financial interests or personal relationships that could have appeared to influence the work reported in this paper.

Acknowledgements

The authors are grateful to the laboratory of Dr. Lalit Srivastava for lending us the Ultrasonic Vocalizations equipment, particularly to Teresa Joseph. Additionally, we would like to thank Lourdes de Cossio Fernandez for sharing her protocol for performing the behavioural assays. We would like to thank Drs Bruno Giros and Salah El Mestikawy for lending us their centrifuge. The data used in this manuscript will be made publicly available on the zenodo platform (10.5281/zenodo.5188961). Finally, the authors would like to acknowledge their funding bodies, including the Canadian Institute of Health Research and Healthy Brains for Healthy Lives for providing support for this research. Additionally, we would like to thank the Fonds de Recherche du Québec en Santé for providing salary support for EG and MMC, as well as the Kappa Kappa Gamma Foundation of Canada for supporting EG's salary.

Appendix A. Supplementary data

Supplementary data to this article can be found online at https://doi.org/10.1016/j.nicl.2021.102868.

References

Amaral, D.G., Schumann, C.M., Nordahl, C.W., 2008. Neuroanatomy of autism. Trends Neurosci. 31 (3), 137–145.
Arriaga, G., Jarvis, E.D., 2013. Mouse vocal communication system: are ultrasounds learned or innate? Brain Lang. 124 (1), 96–116.
Avants, B.B., Tustison, N.J., Song, G., Cook, P.A., Klein, A., Gee, J.C., 2011. A reproducible evaluation of ANTs similarity metric performance in brain image registration. Neuroimage. 54 (3), 2033–2044.
Baharnoori, M., Bhardwaj, S.K., Srivastava, L.K., 2012. Neonatal behavioral changes in rats with gestational exposure to lipopolysaccharide: a prenatal infection model for developmental neuropsychiatric disorders. Schizophr Bull. 38 (3), 444–456.
Barron, H.C., Mars, R.B., Dupret, D., Lerch, J.P., Sampaio-Baptista, C., 2021. Cross-species neuroscience: closing the explanatory gap. Philosophical Transactions of the Royal Society of London: Biological Sciences 376 (1815).
Bates, D., Mächler, M., Bolker, B., Walker, S., 2015. Fitting Linear Mixed-Effects Models Usinglme4 [Internet]. Available from Journal of Statistical Software Vol. 67. https://doi.org/10.18637/jss.v067.i01.
M D Bauman A-M Iosif P Ashwood D Braunschweig A Lee C M Schumann J Van de Water D G Amaral Maternal antibodies from mothers of children with autism alter brain growth and social behavior development in the rhesus monkey Transl Psychiatry. 3 7 2013 e278 e278.
Boksa, P., 2010. Effects of prenatal infection on brain development and behavior: a review of findings from animal models. Brain Behav Immun. 24 (6), 881–897.
Brown, A.S., Meyer, U., 2018. Maternal Immune Activation and Neuropsychiatric Illness: A Translational Research Perspective. Am J Psychiatry. 175 (11), 1073–1083.
Brown, A.S., Cohen, P., Harkavy-Friedman, J., Babulas, V., Malaspina, D., Gorman, J.M., Susser, E.S., 2001. Prenatal rubella, premorbid abnormalities, and adult schizophrenia. Biol Psychiatry. 49 (6), 473–486.
Brown, A.S., Begg, M.D., Gravenstein, S., Schaefer, C.A., Wyatt, R.J., Bresnahan, M., Babulas, V.P., Susser, E.S., 2004. Serologic evidence of prenatal influenza in the etiology of schizophrenia. Arch Gen Psychiatry. 61 (8), 774. https://doi.org/10.1001/archpsyc.61.8.774.
Branchi, I., Ricceri, L., 2002. Transgenic and knock-out mouse pups: the growing need for behavioral analysis. Genes Brain Behav. 1 (3), 135–141.
Cesar P Canales Myka L Estes Karol Cichewicz Kartik Angara John Paul Aboubechara Scott Cameron Kathryn Prendergast Linda Su-Feher Iva Zdilar Ellie J Kreun Emma C Connolly Jin Myeong Seo Jack B Goon Kathleen Farrelly Tyler W Stradleigh Deborah van der List Lori Haapanen Judy Van de Water Daniel Vogt A Kimberley McAllister Alex S Nord 10 10.7554/eLife.60100.
Choi GB, Yim YS, Wong H, Kim S, Kim H, Kim SV, et al. The maternal interleukin-17a pathway in mice promotes autism-like phenotypes in offspring [Internet]. Vol. 351, Science. 2016. p. 933–9. Available from: https://doi.org/10.1126/science.aad0314.
Chung, M.K., Worsley, K.J., Paus, T., Cherif, C., Collins, D.L., Giedd, J.N., Rapoport, J.L., Evans, A.C., 2001. A unified statistical approach to deformation-based morphometry. Neuroimage. 14 (3), 595–606.
Crum, W.R., Sawiak, S.J., Chege, W., Cooper, J.D., Williams, S.C.R., Vernon, A.C., 2017. Evolution of structural abnormalities in the rat brain following in utero exposure to maternal immune activation: A longitudinal in vivo MRI study. Brain Behav Immun. 63, 50–59.
Dazai, J., Spring, S., Cahill, L.S., Henkelman, R.M., 2011. Multiple-mouse neuroanatomical magnetic resonance imaging. J Vis Exp 27 (48). https://doi.org/10.3791/2497.
Estes, M.L., McAllister, A.K., 2016. Maternal immune activation: Implications for neuropsychiatric disorders. Science. 353 (6301), 772–777.
Fatemi, S.H., Folsom, T.D., Reutiman, T.J., Huang, H., Oishi, K., Mori, S., 2009. Prenatal viral infection of mice at E16 causes changes in gene expression in hippocampi of the offspring. Eur Neuropsychopharmacol. 19 (9), 648–653.

Feather-Schussler DN, Ferguson TS. A Battery of Motor Tests in a Neonatal Mouse Model of Cerebral Palsy. J Vis Exp [Internet]. 2016 Nov 3;(117). Available from: https://doi.org/10.3791/53569.

Cossío LF de, de Cossío LF, Guzmán A, van der Veldt S, Luheshi GN. Prenatal infection leads to ASD-like behavior and altered synaptic pruning in the mouse offspring [Internet]. Vol. 63, Brain, Behavior, and Immunity. 2017. p. 88–98. Available from: https://doi.org/10.1016/j.bbi.2016.09.028.

Fischer, J., Hammerschmidt, K., 2011. Ultrasonic vocalizations in mouse models for speech and socio-cognitive disorders: insights into the evolution of vocal communication. Genes Brain Behav. 10 (1), 17–27.

Ginsberg, Y., Khatib, N., Weiner, Z., Beloosesky, R., 2017 Apr. 28;8(2). Available from: 8 (2), e0028. https://doi.org/10.5041/RMMJ.2076917210.5041/RMMJ.10305.

Graham, A.M., Rasmussen, J.M., Rudolph, M.D., Heim, C.M., Gilmore, J.H., Styner, M., Potkin, S.G., Entringer, S., Wadhwa, P.D., Fair, D.A., Buss, C., 2018. Maternal Systemic Interleukin-6 During Pregnancy Is Associated With Newborn Amygdala Phenotypes and Subsequent Behavior at 2 Years of Age. Biol Psychiatry. 83 (2), 109–119.

Guma E, Bordeleau M, Snook E, Desrosiers-Grégoire G, Ibáñez FG, Picard K, et al. Differential effects of early or late exposure to prenatal maternal immune activation on mouse embryonic neurodevelopment [Internet]. bioRxiv. 2021 [cited 2021 Aug 11]. p. 2021.07.14.452084. Available from: https://www.biorxiv.org/content/10.1101/2021.07.14.452084v2.

Guma E, Bordignon P do C, Devenyi GA, Gallino D, Anastassiadis C, Cvetkovska V, et al. Early or late gestational exposure to maternal immune activation alters neurodevelopmental trajectories in mice: an integrated neuroimaging, behavioural, and transcriptional study. Biol Psychiatry [Internet]. 2021 Mar 22; Available from: https://doi.org/10.1016/j.biopsych.2021.03.017.

Guma E, Plitman E, Chakravarty MM. The role of maternal immune activation in altering the neurodevelopmental trajectories of offspring: A translational review of neuroimaging studies with implications for autism spectrum disorder and schizophrenia. Neurosci Biobehav Rev [Internet]. 2019; Available from: https://www.sciencedirect.com/science/article/pii/S0149763419302088.

Gumusoglu, S.B., Stevens, H.E., 2019. Maternal Inflammation and Neurodevelopmental Programming: A Review of Preclinical Outcomes and Implications for Translational Psychiatry. Biol Psychiatry. 85 (2), 107–121.

Gzielo, K., Potasiewicz, A., Litwa, E., Piotrowska, D., Popik, P., Nikiforuk, A., 2021 Mar 9. The Effect of Maternal Immune Activation on Social Play-Induced Ultrasonic Vocalization in Rats. Brain Sciences. 11 (3), 344.

Inui, T., Kumagaya, S., Myowa-Yamakoshi, M., 2017. Neurodevelopmental Hypothesis about the Etiology of Autism Spectrum Disorders. Front Hum Neurosci. 11 (11), 354.

Jiménez, J.A., Zylka, M.J., 2021 Jan 4. Controlling litter effects to enhance rigor and reproducibility with rodent models of neurodevelopmental disorders. J Neurodev Disord. 13 (1), 2.

Kannan, S., Saadani-Makki, F., Balakrishnan, B., Chakraborty, P., Janisse, J., Lu, X., et al., 2011. Magnitude of [(11)C]PK11195 binding is related to severity of motor deficits in a rabbit model of cerebral palsy induced by intrauterine endotoxin exposure. Dev Neurosci. 33 (3–4), 231–240.

Kannan, S., Saadani-Makki, F., Balakrishnan, B., Dai, H., Chakraborty, P.K., Janisse, J., Muzik, O., Romero, R., Chugani, D.C., 2011. Decreased cortical serotonin in neonatal rabbits exposed to endotoxin in utero. J Cereb Blood Flow Metab. 31 (2), 738–749.

Kentner, A.C., Bilbo, S.D., Brown, A.S., Hsiao, E.Y., McAllister, A.K., Meyer, U., Pearce, B. D., Pletnikov, M.V., Yolken, R.H., Bauman, M.D., 2019. Maternal immune activation: reporting guidelines to improve the rigor, reproducibility, and transparency of the model. Neuropsychopharmacology. 44 (2), 245–258.

Knuesel, I., Chicha, L., Britschgi, M., Schobel, S.A., Bodmer, M., Hellings, J.A., Toovey, S., Prinssen, E.P., 2014. Maternal immune activation and abnormal brain development across CNS disorders. Nat Rev Neurol. 10 (11), 643–660.

Kreitz, S., Zambon, A., Ronovsky, M., Budinsky, L., Helbich, T.H., Sideromenos, S., Ivan, C., Konerth, L., Wank, I., Berger, A., Pollak, A., Hess, A., Pollak, D.D., 2020. Maternal immune activation during pregnancy impacts on brain structure and function in the adult offspring. Brain Behav Immun. 83, 56–67.

Lerch, J.P., Gazdzinski, L., Germann, J., Sled, J.G., Henkelman, R.M., Nieman, B.J., 2012. Wanted dead or alive? The tradeoff between in-vivo versus ex-vivo MR brain imaging in the mouse. Front Neuroinform. 23 (6), 6.

Lerch, Jason P, Sled, John G, Henkelman, Mark R, 2011. MRI phenotyping of genetically altered mice. Methods in Molecular Biology 711, 349–361.

Malkova, N.V., Yu, C.Z., Hsiao, E.Y., Moore, M.J., Patterson, P.H., 2012. Maternal immune activation yields offspring displaying mouse versions of the three core symptoms of autism. Brain Behav Immun. 26 (4), 607–616.

McIntosh, A.R., Mišić, B., 2013. Multivariate statistical analyses for neuroimaging data. Annu Rev Psychol. 64 (1), 499–525.

McIntosh, A.R., Lobaugh, N.J., 2004. Partial least squares analysis of neuroimaging data: applications and advances. Neuroimage. 23 (Suppl 1), S250–S263.

Mueller, F.S., Richetto, J., Hayes, L.N., Zambon, A., Pollak, D.D., Sawa, A., Meyer, U., Weber-Stadlbauer, U., 2019. Influence of poly(I:C) variability on thermoregulation, immune responses and pregnancy outcomes in mouse models of maternal immune activation. Brain Behav Immun. 80, 406–418.

Mueller, F.S., Scarborough, J., Schalbetter, S.M., Richetto, J., Kim, E., Couch, A., Yee, Y., Lerch, J.P., Vernon, A.C., Weber-Stadlbauer, U., Meyer, U., 2021. Behavioral, neuroanatomical, and molecular correlates of resilience and susceptibility to maternal immune activation. Mol Psychiatry. 26 (2), 396–410.

Patel, R.T., Gallamoza, B.M., Kulkarni, P., Sherer, M.L., Haas, N.A., Lemanski, E., Malik, I., Hekmatayr, K., Parcells, M.S., Schwarz, J.M., 2021. An Examination of the Long-Term Neurodevelopmental Impact of Prenatal Zika Virus Infection in a Rat Model Using a High Resolution, Longitudinal MRI Approach. Viruses, 13 (6).

Qiu, L.R., Fernandes, D.J., Szulc-Lerch, K.U., Dazai, J., Nieman, B.J., Turnbull, D.H., Foster, J.A., Palmert, M.R., Lerch, J.P., 2018. Mouse MRI shows brain areas relatively larger in males emerge before those larger in females. Nat Commun. 9 (1) https://doi.org/10.1038/s41467-018-04921-2.

Reisinger, S., Khan, D., Kong, E., Berger, A., Pollak, A., Pollak, D.D., 2015 May. The Poly (I:C)-induced maternal immune activation model in preclinical neuropsychiatric drug discovery. Pharmacol Ther. 1 (149), 213–226.

Juliet Richetto Robert Chesters Annamaria Cattaneo Marie A. Labouesse Ana Maria Carrillo Gutierrez Tobias C. Wood Alessia Luoni Urs Meyer Anthony Vernon Marco A. Riva Genome-Wide Transcriptional Profiling and Structural Magnetic Resonance Imaging in the Maternal Immune Activation Model of Neurodevelopmental Disorders 10.1093/cercor/bhw320.

Rousselet, G.A., Pernet, C.R., Wilcox, R.R., 2017. Beyond differences in means: robust graphical methods to compare two groups in neuroscience. Eur J Neurosci. 46 (2), 1738–1748.

Rudolph, M.D., Graham, A.M., Feczko, E., Miranda-Dominguez, O., Rasmussen, J.M., Nardos, R., Entringer, S., Wadhwa, P.D., Buss, C., Fair, D.A., 2018. Maternal IL-6 during pregnancy can be estimated from newborn brain connectivity and predicts future working memory in offspring. Nat Neurosci. 21 (5), 765–772.

Scattoni, M.L., Crawley, J., Ricceri, L., 2009. Ultrasonic vocalizations: a tool for behavioural phenotyping of mouse models of neurodevelopmental disorders. Neurosci Biobehav Rev. 33 (4), 508–515.

L D Selemon N Zecevic Schizophrenia: a tale of two critical periods for prefrontal cortical development Transl Psychiatry. 5 8 2015 e623 e623.

Semple, B.D., Blomgren, K., Gimlin, K., Ferriero, D.M., Noble-Haeusslein, L.J., 2013. Brain development in rodents and humans: Identifying benchmarks of maturation and vulnerability to injury across species. Prog Neurobiol. 106-107, 1–16.

Selten, J.P., van Duursen, R., van der Graaf, Y., Gispen-de Wied, C., Kahn, R.S., 1997. 736 - Second-trimester exposure to maternal stress is a possible risk factor for psychotic illness in the child. Schizophr Res. 24 (1-2), 258. https://doi.org/10.1016/S0920-9964(97)82744-2.

Shen, M.D., Piven, J., 2017 Dec. Brain and behavior development in autism from birth through infancy. Dialogues Clin Neurosci. 19 (4), 325–333.

Short, S.J., Lubach, G.R., Karasin, A.I., Olsen, C.W., Styner, M., Knickmeyer, R.C., Gilmore, J.H., Coe, C.L., 2010. Maternal influenza infection during pregnancy impacts postnatal brain development in the rhesus monkey. Biol Psychiatry. 67 (10), 965–973.

Smolders, S., Smolders, S.M.T., Swinnen, N., Gärtner, A., Rigo, J.-M., Legendre, P., et al., 2015. Maternal immune activation evoked by polyinosinic:polycytidylic acid does not evoke microglial cell activation in the embryo. Front Cell Neurosci. 5 (9), 301.

C.M. Solek N. Farooqi M. Verly T.K. Lim E.S. Ruthazer 247 4 2018 588 619.

Spann, M.N., Monk, C., Scheinost, D., Peterson, B.S., 2018. Maternal Immune Activation During the Third Trimester Is Associated with Neonatal Functional Connectivity of the Salience Network and Fetal to Toddler Behavior. J Neurosci. 38 (11), 2877–2886.

Thion, M.S., Ginhoux, F., Garel, S., 2018. Microglia and early brain development: An intimate journey. Science. 362 (6411), 185–189.

Francesca Melancia Sara Schiavi Michela Servadio Veronica Cartocci Patrizia Campolongo Maura Palmery Valentina Pallottini Viviana Trezza 175 18 2018 3699 3712.

Urbanus, B.H.A., Peter, S., Fisher, S.E., De Zeeuw, C.I., 2020. Region-specific Foxp2 deletions in cortex, striatum or cerebellum cannot explain vocalization deficits observed in spontaneous global knockouts. Sci Rep. 10 (1), 21631.

T.C. Wood M.E. Edye M.K. Harte J.C. Neill E.P. Prinssen A.C. Vernon Mapping the impact of exposure to maternal immune activation on juvenile Wistar rat brain macro- and microstructure during early post-natal development Brain Neurosci Adv. 1 3 2019 Jan 2398212819883086.

Marie Pierre Manitz Manuela Esslinger Simone Wachholz Jennifer Plümper Astrid Friebe Georg Juckel Rainer Wolf 143 1 2013 221 222.

Xia, C.H., Ma, Z., Ciric, R., Gu, S., Betzel, R.F., Kaczkurkin, A.N., Calkins, M.E., Cook, P. A., García de la Garza, A., Vandekar, S.N., Cui, Z., Moore, T.M., Roalf, D.R., Ruparel, K., Wolf, D.H., Davatzikos, C., Gur, R.C., Gur, R.E., Shinohara, R.T., Bassett, D.S., Satterthwaite, T.D., 2018. Linked dimensions of psychopathology and connectivity in functional brain networks. Nat Commun. 9 (1) https://doi.org/10.1038/s41467-018-05317-y.

Zeighami, Y., Fereshtehnejad, S.-M., Dadar, M., Collins, D.L., Postuma, R.B., Mišić, B., Dagher, A., 2019. A clinical-anatomical signature of Parkinson's disease identified with partial least squares and magnetic resonance imaging. Neuroimage. 190, 69–78.

Zhang, Z., Jyoti, A., Balakrishnan, B., Williams, M., Singh, S., Chugani, D.C., Kannan, S., 2018. Trajectory of inflammatory and microglial activation markers in the postnatal rabbit brain following intrauterine endotoxin exposure. Neurobiol Dis. 111, 153–162.